POLITECNICO DI TORINO
Repository ISTITUZIONALE

Membrane/electrolyte interplay on ammonia motion inside a flow-cell for electrochemical nitrogen and nitrate reduction

Original
Membrane/electrolyte interplay on ammonia motion inside a flow-cell for electrochemical nitrogen and nitrate reduction / Pirrone, N.; Garcia Ballesteros, S.; Hernández, S.; Bella, F.. - In: ELECTROCHIMICA ACTA. - ISSN 0013-4686. - ELETTRONICO. - 493:(2024), pp. 1-12. [10.1016/j.electacta.2024.144415]

Availability:
This version is available at: 11583/2991098 since: 2024-07-22T13:01:14Z

Publisher:
Elsevier

Published
DOI:10.1016/j.electacta.2024.144415

Terms of use:

This article is made available under terms and conditions as specified in the corresponding bibliographic description in the repository

Publisher copyright

(Article begins on next page)

07 May 2026

Electrochimica Acta 493 (2024) 144415

Contents lists available at ScienceDirect

Electrochimica Acta

journal homepage: www.journals.elsevier.com/electrochimica-acta

Membrane/electrolyte interplay on ammonia motion inside a flow-cell for electrochemical nitrogen and nitrate reduction

Noemi Pirrone [a], Sara Garcia-Ballesteros [a,*], Simelys Hernández [b], Federico Bella [a,*]

[a] Electrochemistry group, Department of Applied Science and Technology, Politecnico di Torino, C.so Duca degli Abruzzi, 24, Turin 10129, Italy
[b] CREST group, Department of Applied Science and Technology, Politecnico di Torino, C.so Duca degli Abruzzi, 24, Turin 10129, Italy

ARTICLE INFO

Keywords:
Ammonia electrosynthesis
Cation exchange Nafion membrane
Celgard membrane
Ammonium crossover
Flow-cell reactor

ABSTRACT

Electrochemical ammonia production from molecular nitrogen and nitrate reduction reactions at ambient conditions has gained a lot of attention in recent years, making this topic more and more appealing. The race towards good and quick results in terms of Faradaic efficiency and productivity is not always focused on the possible source of ammonia contamination. In particular, Nafion membrane is the most commonly used in this field as cell separator, discarding the possible known disadvantages coming from ammonium ions absorption and release. The wettable microporous Celgard membrane has been proposed as a substitute for Nafion membranes, despite the separation mechanism, in this case, is only dimension-driven, so it does not assure ammonium ions retention. This paper reveals that the mechanism of ammonium ions absorption and release by Nafion 117 is strongly related to the cations present in the electrolyte and to a lesser extent by its pH value. On the other hand, Celgard membrane does not show any relevant ammonium ions absorption. Moreover, the different trend of ammonium ions motion from catholyte to anolyte solution inside a flow-cell reactor shows that none of the membranes is able to avoid ammonium ions crossover and that there is a correlation between the applied potential and the motion trend. Electrochemical nitrogen and nitrate reduction tests confirm how Nafion membrane can have a big impact on the final result of ammonium ions production, especially when dealing with low production quantities, leading to mistakes in the real quantity of ammonium ions coming from the reduction reaction.

1. Introduction

Ammonia (NH_3) is a backbone source of nitrogen fertilisers playing a crucial role in global agriculture and food production, and with an annual production of *ca.* 150 Mt is the second largest manufactured chemical. In fact, NH_3 is estimated to be responsible for the existence of nearly half of the world population [1] and its synthesis at the industrial scale is surely the biggest scientific discovery of the 20th century [2]. In recent years, due to its peculiar properties (*i.e.*, high energy density equal to 4.32 kWh L^{-1} at liquid state, significant hydrogen content up to 17.6 wt%, and easy liquefaction for handling, storage, and transportation), NH_3 has emerged as a potential fuel on the route towards decarbonisation [3–5]. Several authors even talk about the implementation of a NH_3-based economy in the future [6–9].

Up to now, NH_3 is industrially almost exclusively produced (90%) *via* the Haber-Bosch process, which relies on fossil fuels as the main source of hydrogen (H_2) precursor [10]. This process requires high temperatures (300–500 °C) to off-set the sluggish kinetics of the reaction and high pressures (200–300 atm) to avoid NH_3 decomposition at such elevated temperatures, making each industrial plant highly energy demanding (485 kJ mol^{-1}) [11]. As a consequence, *ca.* 2% of the world energy production is consumed and 400 Mt of carbon dioxide (CO_2) are annually released to the environment. Therefore, approaching an NH_3-based economy makes the development of environmentally friendly and energy-efficient alternative production processes mandatory.

In such a scenario, one approach that holds great potential is the electrochemical NH_3 synthesis under mild conditions based on the nitrogen (N_2) or nitrate (NO_3^-) reduction reactions (E-NRR or E-NO_3RR) [12,13]. Those processes can offer many advantages apart from the obvious elimination of fossil fuels and CO_2 emissions: (1) converting sustainable energy in remote areas to transportable chemicals; (2) smaller plant infrastructure favouring the on-site NH_3 generation and, thus, its decentralisation; (3) E-NO_3RR provides a pathway for

* Corresponding authors.
E-mail addresses: sara.garcia@polito.it (S. Garcia-Ballesteros), federico.bella@polito.it (F. Bella).

https://doi.org/10.1016/j.electacta.2024.144415
Received 14 February 2024; Received in revised form 3 May 2024; Accepted 8 May 2024
Available online 8 May 2024
0013-4686/© 2024 The Authors. Published by Elsevier Ltd. This is an open access article under the CC BY license (http://creativecommons.org/licenses/by/4.0/).

efficiently converting one of the most widespread groundwater pollutant (*i.e.*, NO_3^-) into a high-valued-added product (*i.e.*, NH_3). [12,14,15] Although substantial research work focuses on the study of both E-NRR/E-NO_3RR, they remain in preliminary stages, facing challenges mostly related to the low selectivity of the system, which leads to low efficiencies [16,17]. On the other hand, part of the know-how developed in recent years in the field of CO_2 electroreduction can be precious for the electrochemical conversion of nitrogenous species [18–20].

Among the different electrolytic cells employed to perform E-NRR/E-NO_3RR, the use of divided cells (*e.g.* H-type cell or flow-cells) is considered the most suitable approach, since it minimises the possible re-oxidation at the anode of the reduced species from the cathode. [21] In those systems, catholyte and anolyte are usually divided by an ion exchange membrane, being Nafion the most commonly used [22]. Such membranes are made of a poly(tetrafluoroethylene) (PTFE) backbone and sulfonic groups at the side chains, which are actively involved in the proton transport [23]. However, the interaction of Nafion membranes with ammonium ions (NH_4^+) is known and some studies question its use, especially for E-NRR, where the amount of NH_4^+ produced is still low and a minimum source of pollution can easily lead to false positives [22,24–27]. Despite the transport properties of cation-exchange membranes are quite important, with particular relevance to the contamination problems, in-depth understanding of the influence that the membrane and its interactions with the electrolyte have in the E-NRR/E-NO_3RR have not yet received enough attention.

On the other side, Celgard membranes have always been employed for energy storage device separators [28–31]. Contrary to Nafion membranes, such separators have a microporous structure, commonly made in poly(propylene) and poly(ethylene). The transport mechanism does not involve an interaction between the species in the electrolyte and the structure of the membrane itself, making it free from any possible contaminations [32,33]. For such property, this separator became attractive for the world of E-NRR and E-NO_3RR, and it was proposed as a substitute for Nafion membranes in the rigorous protocol for electrochemical NH_3 synthesis published in 2019 by Andersen et al [25]. Since then, the number of works employing Celgard membranes as separators has increased in both E-NRR and E-NO_3RR applications [34–38]. However, information regarding its influence on the system and how NH_4^+ can migrate between anolyte and catholyte is still missing.

Some studies addressing the membrane-NH_4^+ interaction in E-NRR/E-NO_3RR systems can be found in the literature [22,25,27,39–42]. For example, in the context of this work, Leonardi et al. [42] compared the NH_4^+ uptake by Nafion and Zifron membranes in NH_4^+ enriched water and Na_2SO_4 0.1 M electrolyte (pH 6.5) and transport inside an H-type cell; Gyenge et al. [40] employed Nafion membranes of different thicknesses in combination with three electrolytes at pH values equal to 1 (with H_2SO_4 0.05 M), *ca.* 6 (with Na_2SO_4 0.1 M), and 13 (with NaOH 0.1 M) in a membrane electrode assembly-type electrolytic cell, thus testing the NH_4^+ crossover and volatilization as NH_3. Wilder et al. [39] studied the influence of three different kinds of membranes (*i.e.*, anion exchange membrane, cation exchange membrane, and porous membrane) on the NH_4^+ motion inside two different cell architectures (*i.e.*, H-type and zero-gap gas diffusion electrode (GDE)-type). However, there is still disagreement among the reported results, values for the NH_3 crossover from the catholyte to the anolyte varied from 2% [27] to 25–49% [22,39,40] depending on the cell architecture, membrane thickness, electrolyte pH, *etc*. Moreover, in most of the studies, Na_2SO_4, strong acids (*e.g.* H_2SO_4, HCl) or bases (*e.g.* NaOH) are used as electrolytes and detailed information about how the cation species present in the electrolyte or applied potential can affect the membrane-NH_4^+ interaction is still missing.

This paper aims to give a full understanding of how NH_3 interacts with both Nafion and Celgard membranes, as well as its motion inside a flow-cell reactor during E-NRR and E-NO_3RR. For the first time, the influence of the electrolyte composition (in terms of type of cation and pH) on the membrane-NH_4^+ interaction is assessed. In particular, the dependence of NH_4^+ absorption on the membranes is investigated under different conditions to find whether there is a correlation between the other cationic species present in the solution and the pH, or not. Moreover, the NH_4^+ passage across each membrane inside a flow-cell microreactor (three-chamber configuration) without and with applying a potential has also been considered. Such experiments allow us to have a better understanding of the possible source of NH_4^+ contamination in different operating conditions and the effect they have on the overall NH_4^+ production performance assessment.

2. Experimental

2.1. Materials

Nafion membranes (Nafion 117, N-117) with a nominal thickness of 183 μm were purchased from Quintech. Celgard 3401 separator with nominal thickness of 25 μm was purchased from Celgard.

Anhydrous lithium, sodium, and potassium sulphates (Li_2SO_4, K_2SO_4, and Na_2SO_4, ≥99.0%) were purchased from Sigma-Aldrich and used to prepare electrolytes with a concentration of 0.1 M Sulfuric acid (H_2SO_4, 95.0%−98.0%), used to modify the pH of the solutions, as trap for NH_3, and to activate N-117, potassium hydroxide (≥85.0%), used to modify the pH of the solutions, and hydrogen peroxide (H_2O_2, 30 wt%), used to clean N-117 membrane, were purchased from Sigma-Aldrich. Ammonium chloride (NH_4Cl, 99.99%), used as NH_4^+ source, was also bought from Sigma-Aldrich. Sodium citrate dihydrate ($HOC(COONa)(CH_2COONa)_2{\cdot}2H_2O$, ≥99.0%), sodium salicylate ($C_7H_5NaO_3$, 99.5%), sodium nitroferricyanide(III) dihydrate ($Na_2[Fe(CN)_5NO]{\cdot}2H_2O$, 99.0%), sodium hypochlorite (NaClO, 5% active chlorine), and sodium hydroxide (NaOH, ≥97.0%), used to measure the NH_4^+ concentration in the electrolyte via the salicylate method (described in Section 2.2), were purchased from Sigma-Aldrich. Potassium nitrate (KNO_3, ≥99.0%) was purchased from Sigma-Aldrich and used as nitrate source in E-NO_3RR experiments. Commercial molybdenum disulfide (MoS_2, <2 μm, 99.0%) powder, used as catalyst in E-NRR and E-NO_3RR, was also purchased from Sigma-Aldrich. All the solutions were prepared with ultrapure water (Milli-Q).

2.2. Ammonia quantification

The concentration of NH_4^+ was determined spectrophotometrically by using the salicylate method optimized by Giner-Sanz et al [43]. In a typical way, 2 mL of samples were added with 240 μL of salicylate catalyst solution (2.75 M $C_7H_5NaO_3$ and 0.95 mM $Na_2[Fe(CN)_5NO]{\cdot}2H_2O$), followed by the addition of 400 μL of alkaline NaClO solution (previously prepared by diluting 1:10 the NaClO 5% in a aqueous solution containing $HOC(COONa)(CH_2COONa)_2{\cdot}2H_2O$ 340 mM and NaOH 465 mM). After being kept under dark for 45 min, the absorbence at 650 nm of the mixed samples was measured using a HITACHI U-500 UV spectrophotometer. The concentration was determined according to the calibration lines obtained before (see Figure S1).

2.3. Ammonia absorption/releasing tests

The absorption tests were performed by immersing the membranes (5 × 5 cm size) in a beaker containing 70 mL of Milli-Q water or the studied electrolytes (*i.e.*, K_2SO_4, Na_2SO_4, and Li_2SO_4) and NH_4^+ 2 mg L^{-1} at three different pH values (*i.e.*, 3.5, 7.0, and 11.0) for 24 h. The salt concentration for all the electrolytes was 0.1 M and the pH was adjusted to the desired value by dropwise addition of diluted H_2SO_4 or KOH. Regarding the desorption tests, the previously absorbed membranes were immersed for another 24 h in 70 mL of fresh solutions (Milli-Q water, K_2SO_4, Na_2SO_4, and Li_2SO_4). In both cases, samples were periodically taken and analysed to monitor the NH_4^+ concentration evolution.

Before tests, N-117 membranes were activated following a

commonly used method consisting of 3 boiling steps at *ca.* 80 °C in 3 wt % H_2O_2 for 1 h, then in Milli-Q water, and finally in H_2SO_4 0.5 M, rinsing between and after the boiling step with Milli-Q water.

2.4. Electrochemical setup and measurements

A commercial micro-flow-cell reactor (ElectroCell A/S) equipped with a GDE and assembled in a three-chambers configuration (*i.e.*, gas and liquid on the cathodic side, liquid in the anodic one, see Figure S2) was used for NH_4^+ motion experiments and E-NRR/E-NO_3RR tests. When needed, the electrochemical tests were performed with a VSP-300 potentiostat (Biologic). The electrode area was 10.2 cm^2 and the distance between the electrode and the membrane was 6.2 mm. The membranes were placed as the separator of the two liquid chambers. The respective electrolytes (*i.e.*, K_2SO_4, Na_2SO_4, or Li_2SO_4) were continuously recirculated from reservoir bottles through a peristaltic pump at a flow rate of 20 mL min^{-1}. The catholyte and anolyte total volume was 50 mL and reservoir bottles were sealed to avoid possible NH_3 losses, especially when working under alkaline conditions. For NH_4^+ motion experiments, 2 mg L^{-1} of NH_4^+ were added to the catholyte reservoir bottle. All the experiments lasted for 3 h and samples were periodically taken from both catholyte and anolyte to monitor the NH_4^+ concentration; after the tests, membranes were immersed in fresh electrolyte to desorb the possible absorbed NH_4^+, and the liquid was analysed after 24 h. When no potential was applied to the cell, a bare carbon paper (Toray, 0.19 mm thickness - 20 wt% PTFE treated) was placed as working electrode (WE). Instead, the tests conducted applying a potential difference were carried out employing a GDE consisting of commercial MoS_2 catalyst deposited on the carbon paper through air-brushing. Commercial MoS_2 was chosen as active material; indeed, even if it is not the best catalyst for E-NRR/E-NO_3RR due to its intrinsic catalytic activity for water reduction, it is still expected to be active towards E-NRR/E-NO_3RR, considering that molybdenum and sulphur play key roles in N_2 fixation [44]. The counter electrode (CE) at the anode was a mixed metal oxide electrode with iridium, while a leak-free Ag/AgCl electrode, placed close to the cathode (at 5 mm), was used as reference electrode. Ar or N_2 gas (purity 99.9999%), further purified by passing through a commercial filter (Agilent) following an already published procedure [45], were supplied at 5 mL min^{-1} in the gas chamber at the back side of the cathode, to allow a simpler release of the gaseous products (H_2 and NH_3).

All electrochemical NH_4^+ synthesis (E-NRR and E-NO_3RR) studies were performed according to the following protocol: (i) open circuit voltammetry (OCV) until reaching stability; (ii) cyclic voltammetry (CV) at a scan rate of 10 mV s^{-1} and linear sweep voltammetry (LSV) at 5 mV s^{-1} within 0 and −2 V *vs* Ag/AgCl; (iii) chronoamperometry (CA) or chronopotentiometry (CP) at the selected potential or current density; (iv) OCV until reaching stability again. For E-NRR, steps (i) and (ii) were carried out first with Ar and then again under N_2. The full protocol was repeated using only Ar atmosphere as a control test. Samples were taken at the beginning, after the LSV (ii), and after the last OCV (iv) from both cathodic and anodic sides, and membranes were immersed in fresh electrolyte to desorb the possible absorbed NH_4^+. In the case of E-NRR, the sample called "background" refers to a sample taken after (i) and (ii) steps in Ar (protocol scheme in Figure S3). Moreover, in those experiments, a trap consisting of 20 mL of H_2SO_4 0.02 M was placed in the gas exit to recover possible volatilised NH_3. The total height of the 20 mL acid trap was 5 cm and it was open to air, thus no back-pressure was applied to the cell. E-NO_3RR was performed in K_2SO_4 0.1 M + KNO_3 0.01 M as catholyte and K_2SO_4 0.1 M as anolyte, while E-NRR was performed in K_2SO_4 0.1 M both as catholyte and anolyte. All electrolytes were saturated with Ar before entering the cell.

Faradaic efficiency (FE) and productivity (P) were used as figures of merit to assess the system performance. FE is defined as follows:

$$FE = \frac{n_{NH_3} \cdot F \cdot n_{e^-}}{Q}$$

where n_{NH_3} is the quantity of NH_3 produced (mol), F is the Faraday's constant, n_{e^-} is the number of electrons needed to produce a mole of NH_3 (*i.e.*, 3 mol of e^- per mol NH_3 for E-NRR, 8 mol of e^- per mol NH_3 for E-NO_3RR), and Q is the total charge applied (C). The NH_4^+ considered for FE calculations is that produced during the CA or CP, disregarding that produced during the CV and LSV. Instead, P is defined as:

$$P = \frac{n_{NH_3}}{t}$$

where t is the reaction time, expressed in h.

2.5. Conductivity measurements

Conductivity of N-117 membranes as a function of the electrolyte used was measured through electrochemical impedance spectroscopy (EIS) technique. The membranes were cut into 1 cm diameter disks using a manual puncher. Then, they were cleaned in H_2SO_4 1 M solution in an ultrasonic bath for 1 h and rinsed with Milli-Q water. Before electrochemical testing, membranes were ion-exchanged in the desired solution in an orbital mixer for 7 days changing the solution to a fresh one every 3 days. In particular, it was chosen to compare the conductivity of the membranes exchanged in Milli-Q, Li_2SO_4, K_2SO_4, and Na_2SO_4 at 0.1 M concentration with and without NH_4^+ in solution. The measurements were carried out in a symmetrical T-cell (depicted in Figure S4), equipped with a glassy carbon disk as both cathode and anode, supported by a stainless-steel piston. The membrane was dried with a paper to remove the excess electrolyte and thickness was measured with a thickness gauge. An oscillating voltage of 10 mV at OCV was applied between the WE and the CE in a frequency range between 100 kHz and 10 mHz. The value of the impedance at high frequency is considered as the resistance of the membrane and conductivity is calculated using the following equation:

$$\kappa = \frac{l}{R_m \cdot A}$$

where κ is the conductivity (mS cm^{-1}), l is membrane thickness (cm), A is the membrane area (given 1 cm diameter, it was 0.78 cm^2), and R_m (Ω) is the membrane resistance, extrapolated from the Nyquist's plot using Zview software. When carrying out these experiments, the operating conditions were maintained the same to have consistency and be able to compare the conductivity in different electrolytes. This work is not focused on proton conductivity calculations and does not pretend to have a precise quantification of that value. The aim is to investigate if the presence of NH_4^+ can affect proton conductivity when compared to the values here obtained when no NH_4^+ is added.

3. Results and discussion

3.1. Ammonium ion absorption/release by Nafion/celgard membranes

The capability of Nafion and Celgard membranes to absorb NH_4^+ ions was first tested in Milli-Q water without any supporting electrolyte (apart from the H_2SO_4 or KOH added to adjust the pH, the total concentrations were never higher than 0.16 mM or 1 mM, respectively) by immersing them in a solution containing 2 mg L^{-1} of NH_4^+. Since pH 11 exceeds the NH_4^+ pK_a (9.25) and NH_4^+ deprotonates into NH_3, which can easily pass into the gas phase, a 24 h control test on NH_4^+ enriched (2 mg L^{-1}) Milli-Q water at pH 11.0 was done to evaluate the NH_3 lost into the gas phase, and a decrease in the NH_4^+ concentration of only 5% was found (see Figure S5). As it can be observed in Fig. 1(a), NH_4^+ concentration decreases up to 86.5% of the initial value for the N-117 membrane, while almost no variations were observed for the Celgard one

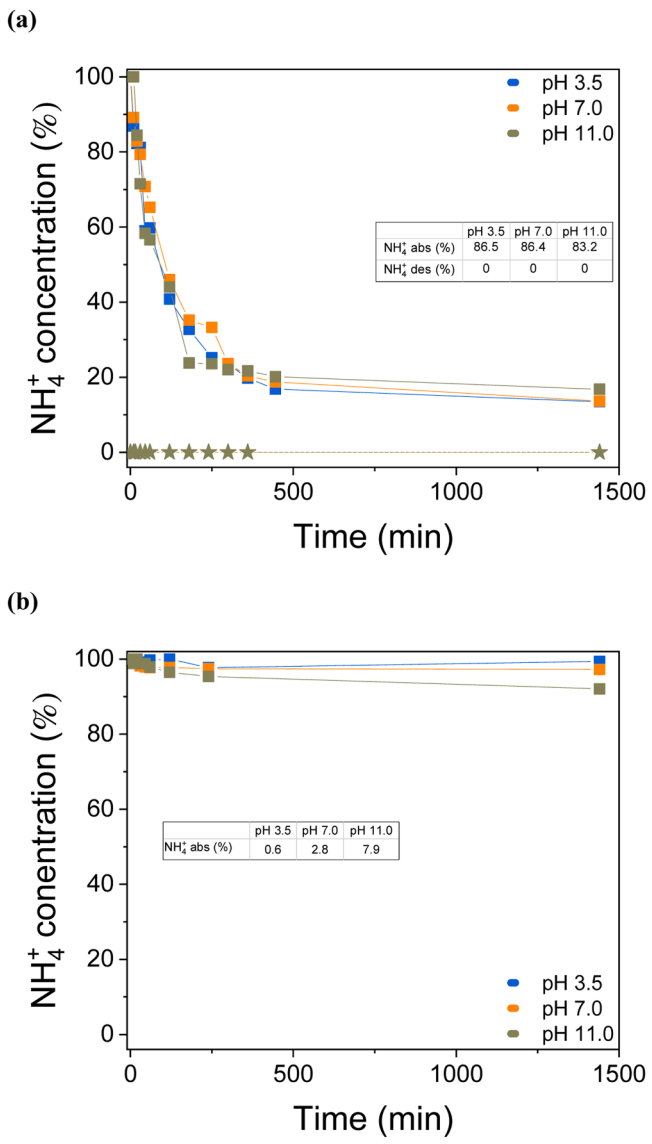

Fig. 1. NH_4^+ absorption in and release from N-117 (a) and Celgard (b) membranes in Milli-Q water at pH 3.5, 7, and 11. NH_4^+ concentration refers to the ratio between NH_4^+ measured at the immersion time *t* and the initial one (2 mg L^{-1}). The solid lines and -■- symbols represent the absorption, while dashed lines and -★- symbol the release. Note that, for Celgard membrane, release test was not done due to the low amount of total NH_3 absorbed on the membrane.

(Fig. 1(b)). Such behaviour is expected considering that N-117 is a cation exchange membrane and Celgard is an inert and size-selective one. These results are thus in line with those already reported in the literature [40,42]. Regarding pH, negligible differences in the NH_4^+ absorption percentage are observed along the test for the three studied values, being the trend after 24 h as follows: absorption at pH 3.5 ≈ 7.0 > 11.0 (Fig. 1(a)). After the absorption, the releasing tests were performed by immersing the previously absorbed membranes in fresh Milli-Q water. As it can be appreciated in Fig. 1(a), no releasing was obtained, since in Milli-Q water no ion exchange can take place. Next, membranes previously absorbed in NH_4^+ enriched (2 mg L^{-1}) Milli-Q water were immersed in fresh electrolytes (*i.e.*, K_2SO_4, Na_2SO_4, and Li_2SO_4 0.1 M) at pH 3.5, 7.0, and 11.0. As shown in Table 1, the amount of NH_4^+ released increases with the atomic radius of the cation in the electrolyte ($Li^+ < Na^+ < K^+$) and the pH value; a release of 89.6% is observed for K_2SO_4 at pH 11, while only a 50.9% of NH_4^+ release is obtained for Li_2SO_4 at pH 3.5. The desorption trend is presented in

Table 1
NH_4^+ absorption-desorption (%) values from N-117 membrane previously absorbed in Milli-Q water containing 2 mg L^{-1} of NH_4^+ at pH 3.5, 7, and 11 and desorbed in Li_2SO_4, Na_2SO_4, and K_2SO_4 0.1 M at pH 3.5, 7, and 11.

	pH 3.5		pH 7.0		pH 11.0	
	%Ass (in H_2O)	%Des	%Ass (in H_2O)	%Des	%Ass (in H_2O)	%Des
Li	88.0	50.9	88.3	55.7	87.7	61.5
Na	88.8	66.5	90.0	78.5	90.0	79.6
K	90.1	82.8	91.3	83.2	92.0	89.6

Figure S6. As for the Celgard membrane, no releasing tests were performed since no NH_4^+ absorption was observed.

To get a deeper understanding of the role that the different cations (*i.e.*, Li^+, Na^+, and K^+) have in the NH_4^+ exchange equilibrium, absorption/release tests were later performed employing all the three electrolytes previously used, again at acidic, neutral, and basic pH (*i.e.*, 3.5, 7.0, and 11.0). Regarding the NH_4^+ absorption, as illustrated in Fig. 2, it decreases with the increase of the ionic radius, namely $Li^+ > Na^+ > K^+$, and the trend is the same independently of the solution pH. Furthermore, NH_4^+ absorption seems to be correlated also to the cation hydration number, which increases in the order $Li^+ > Na^+ > K^+$. It is possible to assume that, when the cation is more solvated by water molecules, it is less reactive with N-117 membrane, facilitating NH_4^+ absorption. On the contrary, when the cation is less solvated by water molecules, it more easily reacts with the membrane, hindering NH_4^+ absorption. Moreover, an oscillation of the NH_4^+ concentration in the first hour of absorption, followed by a stabilization of the value, is observed, meaning that at the beginning the cation in the electrolyte (*i.e.*, Li^+, Na^+ or K^+) and NH_4^+ are in continuous competition for the N-117 membrane sulfonic groups until an equilibrium is reached at *ca.* 180 min. However, for the NH_4^+ release (as previously observed), the opposite trend is obtained, that is, it decreases with increasing the ionic radius. All these results reveal the preference of the membrane for the cations and the increase of this affinity with the ionic radius, as it has been already stated in different works [46–49]. Regarding the pH, a minimal effect with no defined trend on the NH_4^+ absorption and release from N-117 membrane was observed. Regarding adsorption, it generally increases with the decreases of the pH, being the difference higher for Li_2SO_4, while for the desorption no trend was observed. Moreover, a release of 100% of the absorbed NH_4^+ was obtained only when K_2SO_4 0.1 M was employed, confirming the difficulty of removing the NH_4^+ from the N-117 membrane.

Finally, the same experiments were carried out for Celgard membrane, but only for the Li_2SO_4 solution, since it is the one that shows the highest NH_4^+ uptake. As obtained for Milli-Q water experiments, no NH_4^+ absorption was detected after the 24 h immersion, except at pH 11.0 where a decrease of 10% (*ca.* three times lower than with N-117) was obtained (Fig. 3), again confirming the inert character of the membrane.

3.2. *Ammonia motion inside a flow-cell*

The NH_4^+ cross-over from the catholyte to the anolyte employing N-117 and Celgard membranes as separators and the influence of the electrolyte composition were first studied without applying any potential. Since NH_4^+ absorption in batch conditions is more affected by the type of electrolyte than the pH, in the following tests the pH was always neutral and only the effect of the salt cation was studied. Comparing both membranes (Fig. 4), NH_4^+ losses at the cathodic side were similar for N-117 and Celgard, and for different electrolyte solutions, being the decrease only slightly bigger when employing N-117 membrane as separator and Na_2SO_4 and Li_2SO_4 0.1 M as electrolyte. Despite the catholyte NH_4^+ losses are similar for both membranes, the increase at the anodic side is considerably bigger when N-117 (Figure 4(a)) is used as separator. Moreover, membranes were desorbed in fresh electrolytes

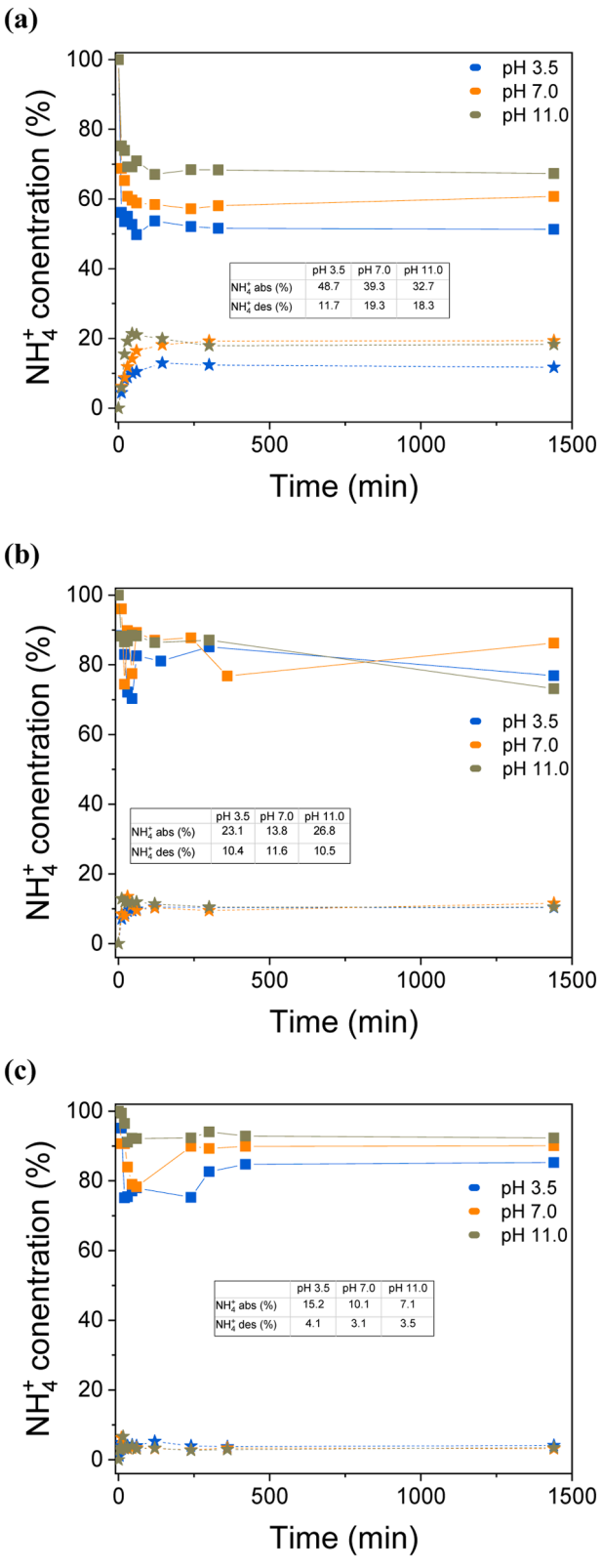

Fig. 2. NH_4^+ absorption in and release from N-117 membrane in Li_2SO_4 0.1 M (a), Na_2SO_4 0.1 M (b), and K_2SO_4 0.1 M (c) electrolytes at pH 3.5, 7, and 11. NH_4^+ concentration refers to the ratio between NH_4^+ measured at the immersion time t and the initial one (2 mg L^{-1}). The solid lines and -■- symbols represent the absorption, while dashed lines and -★- symbol the release.

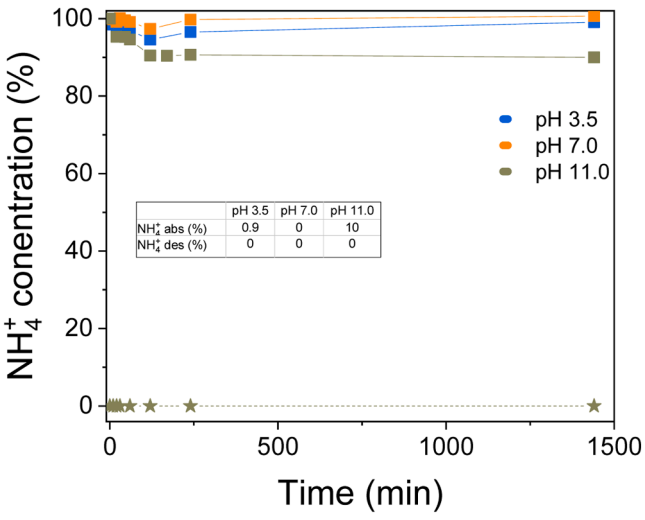

Fig. 3. NH_4^+ absorption in and release from Celgard membrane in Li_2SO_4 0.1 M electrolyte at pH 3.5, 7, and 11. NH_4^+ concentration refers to the ratio between NH_4^+ measured at the immersion time t and the initial one (2 mg L^{-1}). The solid lines and -■- symbols represent the absorption, while dashed lines and -★- symbol the release.

and only N-117 released a considerable amount of NH_4^+. In general, NH_4^+ motion in the case of Celgard membrane - when no potential is applied - is independent of the cation nature, suggesting that NH_4^+ has small enough dimensions to cross Celgard pores and that the concentration gradient is the only driving force.

Finally, if we sum the amount of NH_4^+ found in the different compartments together with the one desorbed from the membrane, the value obtained for N-117 is bigger than the initially added amount, confirming the introduction of NH_4^+ in the system by the N-117, even if they are new and cleaned right before the experiment in H_2SO_4 1 M [22,41]. Additionally, it appears that the NH_4^+ contaminations present in the membrane are released in the anolyte. Such behaviour could be explained by the concentration gradient driving force: NH_4^+ is released in the anolyte within the first 30 min, where the initial concentration of NH_4^+ is zero.

Next, we repeat the same experiments, but applying a low potential commonly adopted in literature for E-NRR/E-NO_3RR, *i.e.*, −1.4 V *vs* Ag/AgCl (J-t curves for these experiments are provided in Figure S7). As illustrated in Fig. 5(b), in the case of Celgard membrane, the NH_4^+ cross-over is higher compared to the case in which no potential is applied (Figure 4(b)), especially when employing Li_2SO_4 0.1 M as electrolyte. Moreover, it seems that, when a slight electric field is applied, a dependence of NH_4^+ motion from the cation shows up, making NH_4^+ motion dependent on electronegativity values of the cation in the electrolyte ($Li^+ > Na^+ > K^+$). Indeed, Li^+ tendency to be attracted towards the negative side (cathode) of the cell is higher, being membrane pores less occupied by Li^+. This aspect, together with the acidification of the anolyte, favours the diffusion of NH_4^+ to the anode. Indeed, Celgard membrane is a porous separator, and no chemical bond arises between the polymer matrix and the cations in the electrolyte. As both NH_4^+ and Li^+ have dimensions small enough to cross that separator, the only driving forces governing the cross-over phenomena are concentration gradient, pH, and electronegativity. Regarding N-117 membrane (Fig. 5 (a)), results are mostly similar to those obtained when no potential is applied, probably because the potential is so low that it does not influence the NH_4^+ motion.

Finally, experiments by increasing the potential to −2 V *vs* Ag/AgCl (Fig. 6) were performed with the K_2SO_4 0.1 M electrolyte; for N-117 membrane, no NH_4^+ crossover was detected. Such results confirm that the NH_4^+ crossover not only depends on the interaction with the membrane itself and the competition with the other cations present in the electrolytes, but also on the applied electrical field; regarding N-117

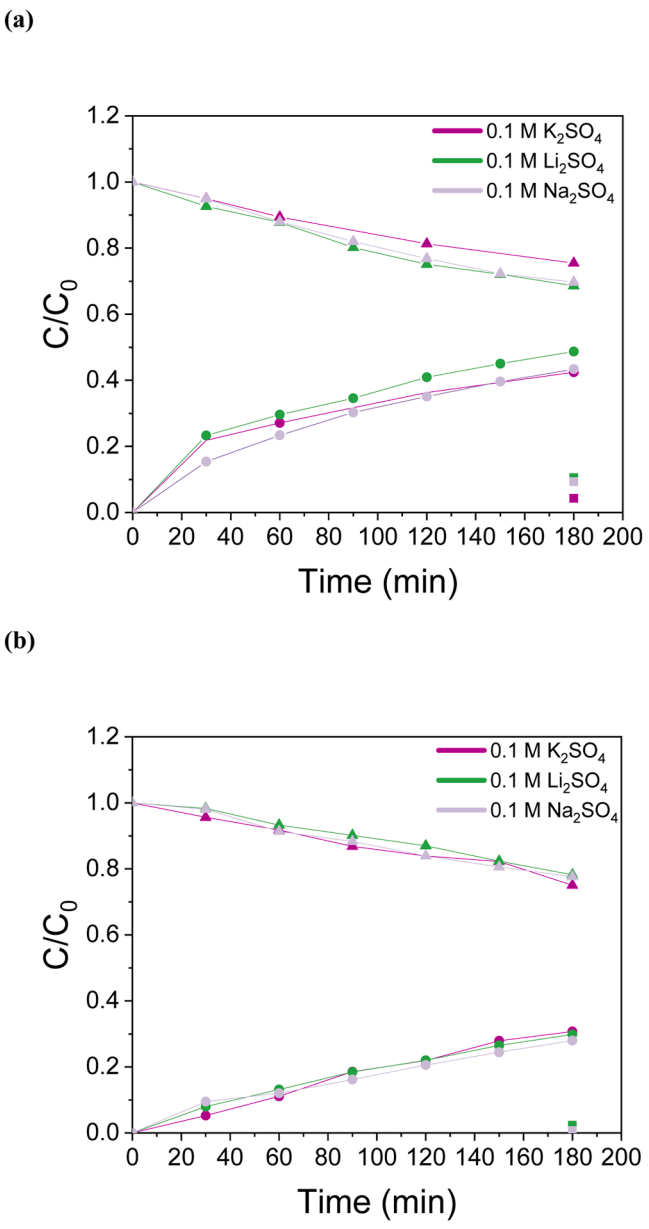

Fig. 4. NH_4^+ motion inside a flow-cell employing different electrolytes without applying any potential, using (a) N-117 and (b) Celgard membranes as separator. The electrolytes tested are Li_2SO_4, Na_2SO_4, and K_2SO_4 with a 0.1 M concentration and a pH value of 7. The initial NH_4^+ concentration is 2 mg L^{-1}. In the plot, (-▲-) is used to identify the cathodic side, while (-●-) is used to identify the anodic side on the cell. (-■-) refers to the NH_4^+ quantity found absorbed on the membrane. That value is the ratio between the quantity found and the initial quantity present in the cathodic side.

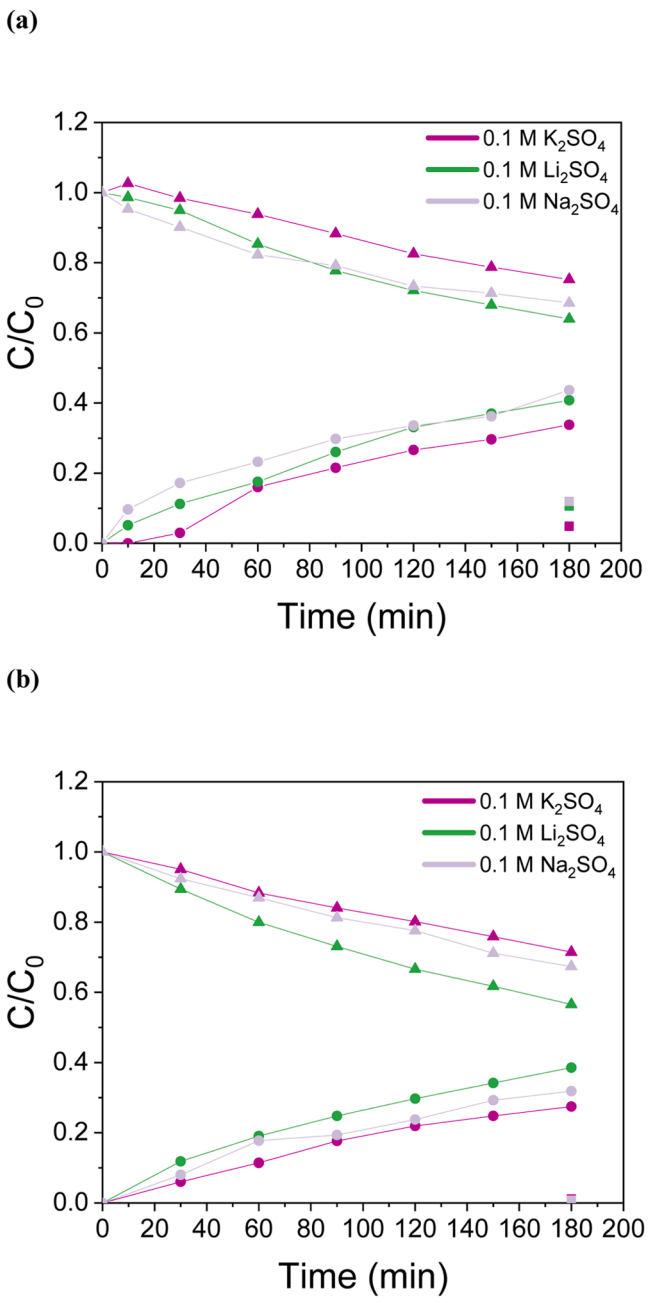

Fig. 5. NH_4^+ motion inside a flow-cell employing different electrolytes during an electrolysis test at −1.4 V *vs* Ag/AgCl for 3 h, employing (a) N-117 and (b) Celgard membranes as separator. The electrolytes tested are Li_2SO_4, Na_2SO_4, and K_2SO_4 with a 0.1 M concentration. The initial NH_4^+ concentration is 2 mg L^{-1}. In the plot, (-▲-) is used to identify the cathodic side, while (-●-) is used to identify the anodic side on the cell. (-■-) refers to the NH_4^+ quantity found absorbed on the membrane. That value is the ratio between the quantity found and the initial quantity present in the cathodic side.

membrane, at increased potential, all positive charges are dragged to the cathodic side charged negatively, overcoming the diffusion across the membrane. On the contrary, in the case of Celgard, the NH_4^+ cross-over increases as the potential increases, until an equilibrium between catholyte and anolyte is reached, as already experienced by Andersen et al [25]. Accordingly, it is not recommended to look at the application of a high potential as a general method to prevent NH_4^+ crossover.

3.3. *E-NO_3RR experiment*

The ability of MoS_2 to convert NO_3^- into NH_4^+ was studied using both N-117 and Celgard membranes. At −1.4 V *vs* Ag/AgCl applied potential for 3 h, the FE and *P* values obtained using the N-117 membrane were 10.6% and 0.79 μmol h^{-1}, respectively, while those obtained using Celgard were 17.6% and 0.85 μmol h^{-1}, respectively. The discrepancy between those values can be attributed to two main factors: (i) the NH_4^+ produced in the case of N-117 is in part absorbed by the membrane, and this amount cannot be considered in the calculations; (ii) in the test using the Celgard membrane, the activity was lower (see LSV and CA plots in Figure S8) and, at the same applied potential, the current density measured was −0.1 mA cm^{-2} on average, while it was −0.16 mA cm^{-2} for N-117. Such a difference in the total charge can have a big impact on the final calculation of the FE for the same amount of NH_4^+ produced.

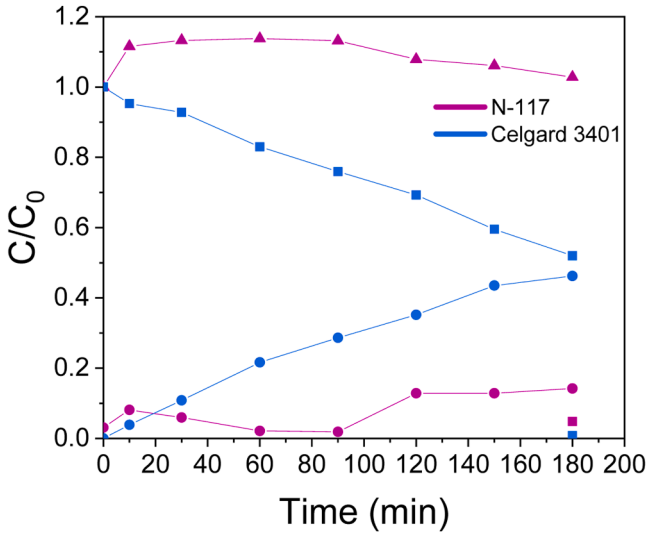

Fig. 6. NH_4^+ motion inside a flow-cell employing K_2SO_4 0.1 M as electrolyte during an electrolysis test at −2 V *vs* Ag/AgCl for 3 h, employing N-117 (purple) and Celgard (blue) membranes as separator. The initial NH_4^+ concentration is 2 mg L^{-1}. In the plot, (-▲-) is used to identify the cathodic side, while (-●-) is used to identify the anodic side on the cell. (-■-) refers to the NH_4^+ quantity found absorbed on the membrane. That value is the ratio between the quantity found and the initial quantity present in the cathodic side.

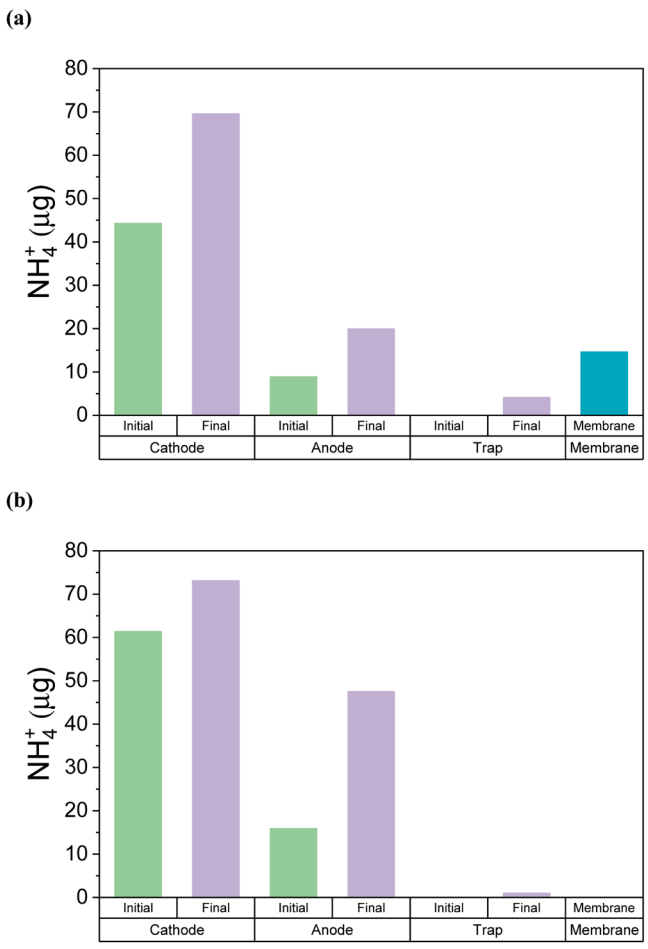

Fig. 7. NH_4^+ produced through E-NO_3RR in a flow-cell reactor, employing MoS_2 as a catalyst in combination with K_2SO_4 0.1 M + KNO_3 0.01 M as electrolyte and (a) N-117 and (b) Celgard membranes as separator. Initial value refers to the quantity of NH_4^+ found in the sample taken after CV and LSV measurements, right before the CA at −1.4 V *vs* Ag/AgCl for 3 h (see Figure S3 for protocol details).

The uncompensated resistance between the WE and reference electrode in the case of N-117 and Celgard were 4.98 Ω and 4.13 Ω, respectively. That difference is negligible and should not affect the resulting current density measured during the CA. In Fig. 7(b) it is possible to see that, in the case of Celgard membrane, NH_4^+ is distributed more uniformly in the anolyte and catholyte, while no NH_4^+ was present on the membrane after the test. On the other side, in the case of N-117, NH_4^+ is much more present in the catholyte side, together with a considerable amount on the membrane itself (Fig. 7(a)).

3.4. E-NRR experiment

The performances of Nafion and Celgard membranes were tested for E-NRR. Unfortunately, MoS_2 commercial catalyst did not show any relevant activity towards NH_4^+ production. Indeed, using both N-117 and Celgard, only a FE equal to 0.02% towards NH_4^+ production was reached at −5 mA cm^{-2} for 2 h, and the control test under argon atmosphere showed the same result, meaning that all the NH_4^+present in the system is coming from ambient contamination.

From Fig. 8(a) we can see that, in the case of N-117, NH_4^+ quantity increases at the cathodic side, but having a look at the anodic one, it is evident that NH_4^+ coming from initial impurities is gradually crossing the membrane, reaching the catholyte chamber. Such behaviour is in agreement with the test on NH_4^+ motion presented in Section 3.2. In this case, NH_4^+ is moving from the anolyte to the catholyte due to the big electric field applied during the test. In addition, having a look at the control test under argon, shown in Fig. 8(b), the difference between the total final and initial NH_4^+ quantity is the same as the one obtained when using N_2, which highlights that no N_2 is effectively reduced to NH_4^+ and all the quantities found come from system impurities.

On the other side, from Fig. 9 it is clear that, using Celgard membrane, the obtained quantities of NH_4^+ are significantly lower than those detected with N-117. In this case, quantities are coherent both under N_2 (Figure 9(a)) and Ar (Fig. 9(b)) environments and remain stable during all the tests. This further confirms that the majority of the contamination is coming from the membrane itself. Even if never used and thoroughly cleaned with H_2SO_4 1 M, the N-117 membrane releases some NH_4^+. It is the authors' opinion that N-117 can absorb NH_3 from the ambient in the time interval needed to assemble the cell. In this framework, Celgard seems to be a good alternative as it is not a source of contamination. However, such a membrane is size-selective, allowing the passage of all the species that have a small enough dimension. Such conditions do not allow the holding of different electrolyte compositions on the catholyte and anolyte sides.

3.5. Effect of cations and NH_4^+ on the conductivity of the Nafion membrane

As previously reported in literature, cations and NH_4^+ can interact with the external sulfonic group of the Nafion chains and contaminate Nafion membranes, hindering the correct proton transport [27]. This phenomenon can affect the overall system not only in terms of NH_4^+ misleading quantification, but also in the control of the bulk pH at the cathode and anode side. Indeed, during the H_2 evolution reaction, H^+ are consumed at the cathode side and local pH rises, while $H^+$are produced at the anode side during O_2 evolution reaction. In an ideal situation, ionic equilibrium should be maintained thanks to proton transport across the cation exchange membrane. However, other species present in the electrolyte can negatively affect proton transport, leading to an increase in the catholyte and a decrease in the anolyte bulk pH. E-NRR and E-NO_3RR have a very strong dependence on the pH [50,51] and such low control on that variable could lead to worse overall

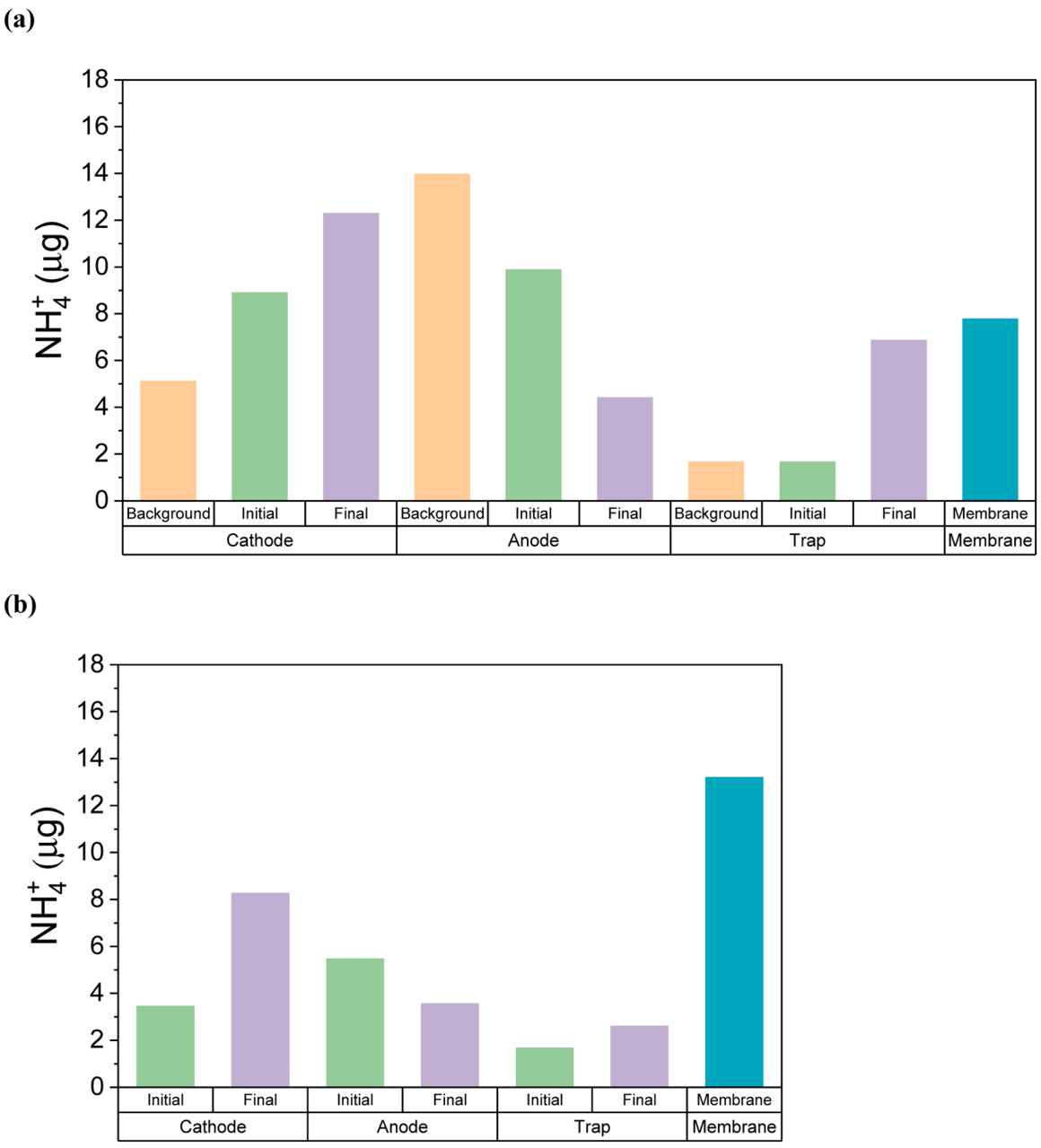

Fig. 8. NH_4^+ produced through E-NRR in a flow-cell reactor, employing MoS_2 as a catalyst in combination with K_2SO_4 0.1 M as electrolyte and N-117 membrane as separator. (a) Test under N_2, background refers to a sample taken after the OCV, LSV, and CV in Ar. Initial value refers to the quantity of NH_4^+ found in the sample taken after CV an LSV measurements under N_2, right before the CP technique at -5 mA cm^{-2} for 2 h (b) Control test under Ar. Initial value refers the sample taken after CV an LSV measurements in Ar, right before the CP at -5 mA cm^{-2} for 2 h (see Figure S3 for protocol details).

performances as well as catalyst stability issues [52,53]. Thus, the purpose of this set of experiments is to assess how proton conductivity of Nafion membrane is affected by the presence of the cations and NH_4^+ in the electrolyte.

The comparison between the conductivity of Nafion membrane exchanged in Li^+, K^+, Na^+, and sole Milli-Q water is presented in Fig. 10. The conductivity decreases up to 83% for the cation-exchanged membrane compared to the proton-exchanged one. The trend shown is in agreement with previous literature data [54] and can be explained through a parallelism with the cation mobility mechanism in water electrolytes: while protons are transported through the hopping mechanism, other cations are transported through the vehicle mechanism, which is slower than the previous one [55].

The variability of conductivity between the different exchanged cations can be explained through the cation correlation with membrane water content, as well as with water molecule mobility inside the membrane [56]. Indeed, as shown in Fig. 10, conductivity decreases in the order $K^+ < Na^+ \leq Li^+$, likewise water uptake trend found in literature, obtained in similar conditions [46]. Moreover, such results are in agreement with Saito et al.'s work. They suggested that water mobility inside the Nafion membrane is affected by the interaction between water molecules and cations present in the solution. Li^+ and Na^+ possess higher interaction with water molecules in the membranes compared to H^+, slowing down water molecules transport through the membrane itself [57]. Conductivity values differ from the ones present in the literature, which are usually in the order of magnitude of 10 mS cm^{-1} [58–60], due to the different experimental setups, but the general trend is maintained. Indeed, the experimental conductivity determination is

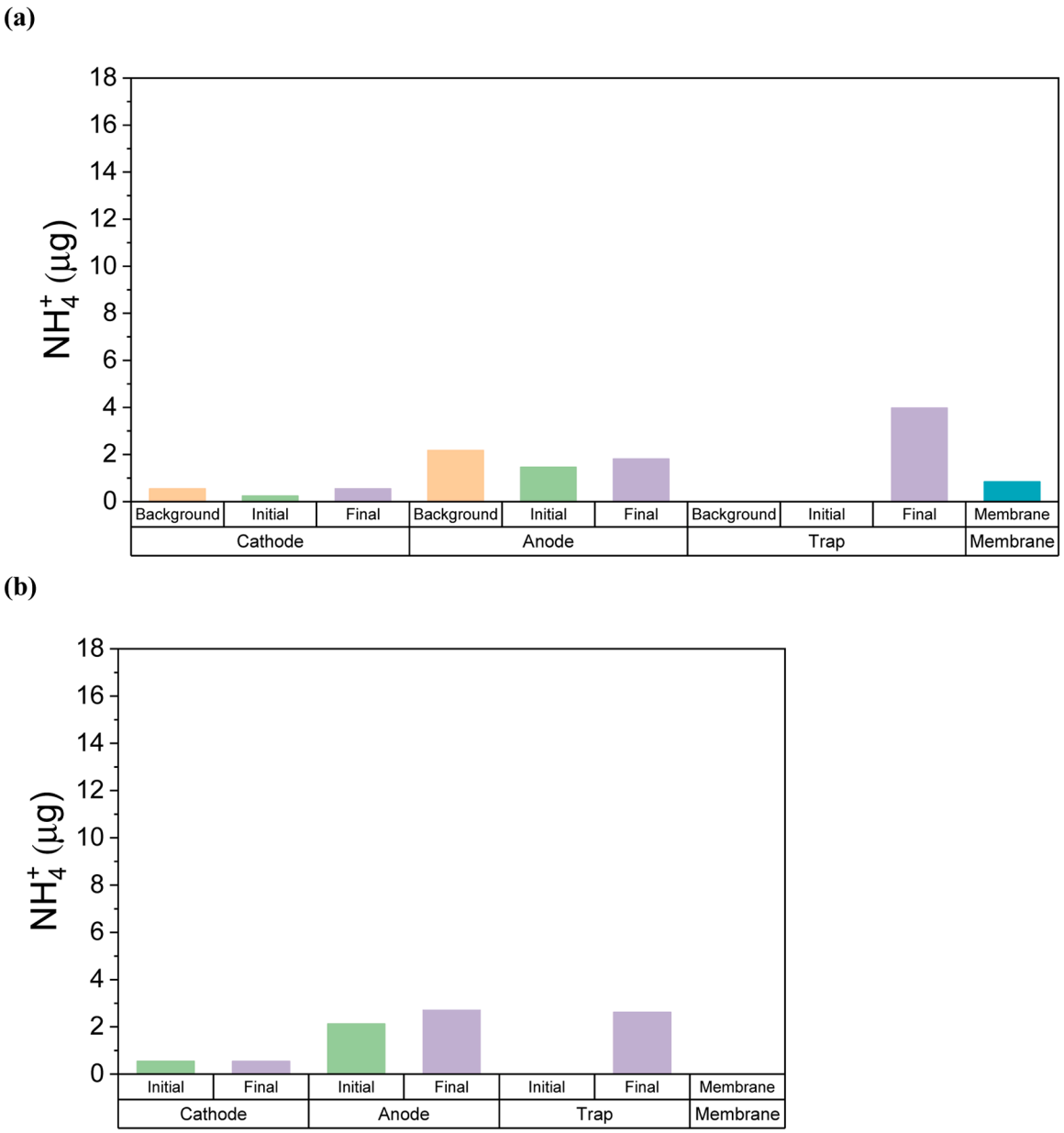

Fig. 9. NH_4^+ produced through E-NRR in a flow-cell reactor, employing MoS_2 as a catalyst in combination with K_2SO_4 0.1 M as electrolyte and Celgard membrane as separator. (a) Test under N_2. Background refers to a sample taken after the OCV, LSV, and CV in Ar. Initial value refers to the quantity of NH_4^+ found in the sample taken after CV an LSV measurements under N_2, right before the CP technique at -5 mA cm^{-2} for 2 h (b) Control test under Ar. Initial value refers to the sample taken after CV an LSV measurements in Ar, right before the CP at -5 mA cm^{-2} for 2 h (see Figure S3 for protocol details).

carried out in low relative humidity conditions, in which conductivity values can be less than 10 mS cm^{-1}, as reported by other studies [61,62]. Moreover, a recent statistical study, that collects all the literature on the topic of proton conductivity of Nafion membranes, clarifies how parameters such as relative humidity and temperature can have a big impact on the final conductivity value [63].

When NH_4^+ is added to the exchanged solution, conductivity is further affected, with a percentage of decrease in the order $Li^+ < Na^+ < K^+$. In the case of K^+, the conductivity decreases in the presence of NH_4^+ is negligible, thus confirming that NH_4^+ poorly interacts with membrane in K^+ containing electrolyte. Such behaviour supports the data on absorption presented till now. Indeed, NH_4^+ absorbed on the Nafion membrane follows the opposite order (*i.e.*, $Li^+ > Na^+ > K^+$), meaning that NH_4^+ has a negative effect on the conductivity with a magnitude strictly dependent on the quantity absorbed.

4. Conclusions

Till now, Nafion 117 and Celgard membranes have been the most commonly used separators for E-NRR and E-NO_3RR experiments, even if they both present some disadvantages. In particular, N-117 is known to absorb NH_4^+, becoming a source of contamination. In this paper, we analysed how different cations (*i.e.*, Li^+, Na^+, and K^+) and pH value in the electrolyte influence the NH_4^+ ions absorbed by N-117 membrane. It seems that 86% of NH_4^+ is absorbed when no cations are present in the solution, while when a cation is added, the absorption values lower to 40, 14, and 10% for Li_2SO_4, Na_2SO_4, and K_2SO_4, respectively, while the pH has no significant effect. Such a trend reflects the increase in the ionic radius as well as the decrease in the cation hydration number, while the trend in NH_4^+ release is the opposite. Contrary to what is stated in other literature works, none of the cations tested can completely exchange the NH_4^+ trapped in N-117. Instead, NH_4^+ is not absorbed by Celgard

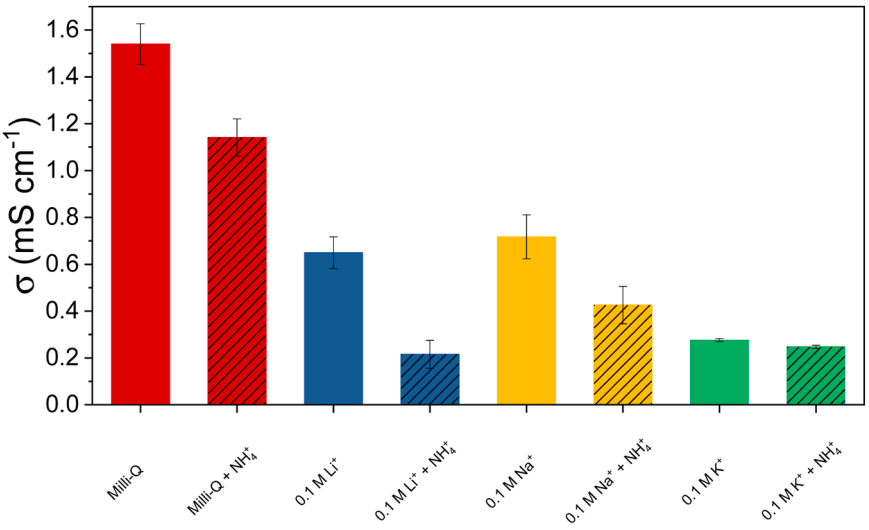

Fig. 10. Conductivity measurements on N-117 membranes exchanged in different electrolytes. Conductivity values are extrapolated from impedance value at high frequency, obtained through EIS. Comparison of all electrolytes in the absence of NH_4^+(solid fill) and with 2 mg L^{-1} of NH_4^+ (pattern fill). The data referred to as Milli-Q are N-117 membranes activated in H_2SO_4 1 M and then exchanged in Milli-Q, which explains the high conductivity.

membrane in any condition.

Then, tests on NH_4^+ motion inside an electrochemical flow-cell reactor revealed that, for N-117 membrane, NH_4^+ motion to the anode side is more prominent in Li_2SO_4, when low potential is applied; conversely, when a potential is applied, the effect of the electric field prevails on the interaction between NH_4^+ and N-117 membrane. On the other side, using Celgard membrane, NH_4^+ motion when no potential is applied is independent from the cation nature, while the application of a potential induces an electric field that moves the equilibrium as a function of the cation electronegativity ($Li^+ > Na^+ > K^+$).

These experiments also demonstrated that N-117 is a big source of contamination, as the final amount of NH_4^+ found in the system was always higher than the initial one. Such contamination was not noticed with Celgard. In addition, E-NRR and E-NO_3RR final tests confirmed that N-117 can lead to false positive and fallacious calculations on the final FE and productivity. Such tests seem to lead to the conclusion that Celgard membranes are the best option for E-NRR and E-NO_3RR, but such separators allow the crossing of multiple species from the catholyte and the anolyte, making it impossible to maintain different environments in the two compartments of the cell.

It is the authors' opinion that much more effort must be focused on the synthesis of a cationic-exchange membrane with specific characteristics for E-NRR and E-NO_3RR applications.

Declaration of competing interest

The authors declare that they have no known competing financial interests or personal relationships that could have appeared to influence the work reported in this paper.

Acknowledgements

This project has received funding from the European Research Council (ERC) under the European Union's Horizon 2020 research and innovation program (grant agreement No. 948769, project title: SuN_2-rise). This study was also carried out within the «HYDREAM» project – funded by European Union - Next Generation EU – within the PRIN 2022 program (D.D. 104 - 02/02/2022 Ministero dell'Università e della Ricerca). Finally, the project was also supported by the European Union's Horizon 2020 research and innovation programme under the Marie Skłodowska-Curie grant agreement No 101107906. This manuscript reflects only the authors' views and opinions, and the Ministry cannot be considered responsible for them.

Supplementary materials

Supplementary material associated with this article can be found, in the online version, at doi:10.1016/j.electacta.2024.144415.

References

[1] D.C. Massuela, S. Munz, J. Hartung, P.M. Nkebiwe, S. Graeff-Hönninger, Cannabis hunger games: nutrient stress induction in flowering stage – impact of organic and mineral fertilizer levels on biomass, cannabidiol (CBD) yield and nutrient use efficiency, Front. Plant Sci. 14 (2023), https://doi.org/10.3389/fpls.2023.1233232.

[2] V. Smil, Detonator of the population explosion, NatureNature 400 (415) (1999) 415, https://doi.org/10.1038/22672.

[3] C. Smith, A.K. Hill, L. Torrente-Murciano, Current and future role of Haber–Bosch ammonia in a carbon-free energy landscape, Energy Environ. Sci. 13 (2020) 331–344, https://doi.org/10.1039/C9EE02873K.

[4] L. Zhai, S. Liu, Z. Xiang, Ammonia as a carbon-free hydrogen carrier for fuel cells: a perspective, Indus. Chem. Mater. 1 (2023) 332–342, https://doi.org/10.1039/D3IM00036B.

[5] S.Joseph Sekhar, M.S. Samuel, G. Glivin, T. Le, T. Mathimani, Production and utilization of green ammonia for decarbonizing the energy sector with a discrete focus on Sustainable Development Goals and environmental impact and technical hurdles, Fuel 360 (2024) 130626, https://doi.org/10.1016/j.fuel.2023.130626.

[6] A. Valera-Medina, F. Amer-Hatem, A.K. Azad, I.C. Dedoussi, M. de Joannon, R. X. Fernandes, P. Glarborg, H. Hashemi, X. He, S. Mashruk, J. McGowan, C. Mounaim-Rouselle, A. Ortiz-Prado, A. Ortiz-Valera, I. Rossetti, B. Shu, M. Yehia, H. Xiao, M. Costa, Review on ammonia as a potential fuel: from synthesis to economics, Energy Fuels 35 (2021) 6964–7029, https://doi.org/10.1021/acs.energyfuels.0c03685.

[7] N. Morlanés, S.P. Katikaneni, S.N. Paglieri, A. Harale, B. Solami, S.M. Sarathy, J. Gascon, A technological roadmap to the ammonia energy economy: current state and missing technologies, Chem. Eng. J. 408 (2021) 127310, https://doi.org/10.1016/j.cej.2020.127310.

[8] E. Spatolisano, L.A. Pellegrini, A.R. de Angelis, S. Cattaneo, E. Roccaro, Ammonia as a carbon-free energy carrier: NH 3 cracking to H 2, Ind. Eng. Chem. Res. 62 (2023) 10813–10827, https://doi.org/10.1021/acs.iecr.3c01419.

[9] D.R. MacFarlane, P.V. Cherepanov, J. Choi, B.H.R. Suryanto, R.Y. Hodgetts, J. M. Bakker, F.M. Ferrero Vallana, A.N. Simonov, A roadmap to the ammonia economy, Joule 4 (2020) 1186–1205, https://doi.org/10.1016/J.JOULE.2020.04.004.

[10] B.H.R. Suryanto, H.L. Du, D. Wang, J. Chen, A.N. Simonov, D.R. MacFarlane, Challenges and prospects in the catalysis of electroreduction of nitrogen to ammonia, Nat. Catal. 2 (2019) 290–296, https://doi.org/10.1038/s41929-019-0252-4.

[11] M.A. Shipman, M.D. Symes, Recent progress towards the electrosynthesis of ammonia from sustainable resources, Catal. Today 286 (2017) 57–68, https://doi.org/10.1016/j.cattod.2016.05.008.

[12] Z.Y.Y. Wu, M. Karamad, X. Yong, Q. Huang, D.A. Cullen, P. Zhu, C. Xia, Q. Xiao, M. Shakouri, F.Y.Y. Chen, J.Y. (Timothy) Kim, Y. Xia, K. Heck, Y. Hu, M.S. Wong, Q. Li, I. Gates, S. Siahrostami, H. Wang, Electrochemical ammonia synthesis via

nitrate reduction on Fe single atom catalyst, Nat. Commun. 12 (2021) 1–10, https://doi.org/10.1038/s41467-021-23115-x.
[13] T. Mou, J. Long, T. Frauenheim, J. Xiao, Advances in electrochemical ammonia synthesis beyond the use of nitrogen gas as a source, Chempluschem. Chempluschem. 86 (2021) 1211–1224, https://doi.org/10.1002/cplu.202100356.
[14] J.G. Chen, R.M. Crooks, L.C. Seefeldt, K.L. Bren, R.M. Bullock, M.Y. Darensbourg, P.L. Holland, B. Hoffman, M.J. Janik, A.K. Jones, M.G. Kanatzidis, P. King, K. M. Lancaster, S.V. Lymar, P. Pfromm, W.F. Schneider, R.R. Schrock, Beyond fossil fuel–driven nitrogen transformations, Science 1979 (2018) 360, https://doi.org/10.1126/science.aar6611.
[15] E. Abascal, L. Gómez-Coma, I. Ortiz, A. Ortiz, Global diagnosis of nitrate pollution in groundwater and review of removal technologies, Sci. Total Environ. 810 (2022) 152233, https://doi.org/10.1016/j.scitotenv.2021.152233.
[16] C.J. Werth, C. Yan, J.P. Troutman, Factors impeding replacement of ion exchange with (Electro)catalytic treatment for nitrate removal from drinking water, ACS. ES. T. Eng. 1 (2021) 6–20, https://doi.org/10.1021/acsestengg.0c00076.
[17] G. Qing, R. Ghazfar, S.T. Jackowski, F. Habibzadeh, M.M. Ashtiani, C.P. Chen, M. R. Smith, T.W. Hamann, Recent advances and challenges of electrocatalytic N 2 reduction to ammonia, Chem. Rev. 120 (2020) 5437–5516, https://doi.org/10.1021/acs.chemrev.9b00659.
[18] Z. Chen, T. Wang, B. Liu, D. Cheng, C. Hu, G. Zhang, W. Zhu, H. Wang, Z.J. Zhao, J. Gong, Grain-boundary-rich copper for efficient solar-driven electrochemical CO $_2$ reduction to ethylene and ethanol, J. Am. Chem. Soc. 142 (2020) 6878–6883, https://doi.org/10.1021/jacs.0c00971.
[19] Y. Mi, Y. Qiu, Y. Liu, X. Peng, M. Hu, S. Zhao, H. Cao, L. Zhuo, H. Li, J. Ren, X. Liu, J. Luo, Cobalt−iron oxide nanosheets for high-efficiency solar-driven CO $_2$ −H $_2$ O coupling electrocatalytic reactions, Adv. Funct. Mater. 30 (2020), https://doi.org/10.1002/adfm.202003438.
[20] X.V. Medvedeva, J.J. Medvedev, S.W. Tatarchuk, R.M. Choueiri, A. Klinkova, Sustainable at both ends: electrochemical CO $_2$ utilization paired with electrochemical treatment of nitrogenous waste, Green Chem. 22 (2020) 4456–4462, https://doi.org/10.1039/D0GC01754J.
[21] S. Garcia-Segura, M. Lanzarini-Lopes, K. Hristovski, P. Westerhoff, Electrocatalytic reduction of nitrate: fundamentals to full-scale water treatment applications, Appl. Catal. B 236 (2018) 546–568, https://doi.org/10.1016/J.APCATB.2018.05.041.
[22] Y. Ren, C. Yu, X. Tan, X. Han, H. Huang, H. Huang, J. Qiu, Is it appropriate to use the Nafion membrane in electrocatalytic N 2 reduction? Small. Methods 3 (2019) https://doi.org/10.1002/smtd.201900474.
[23] P. Choi, N.H. Jalani, R. Datta, Thermodynamics and proton transport in Nafion, J. Electrochem. Soc. 152 (E123) (2005), https://doi.org/10.1149/1.1859814.
[24] C. Tang, S.Z. Qiao, How to explore ambient electrocatalytic nitrogen reduction reliably and insightfully, Chem. Soc. Rev. 48 (2019) 3166–3180, https://doi.org/10.1039/C9CS00280D.
[25] S.Z. Andersen, V. Čolić, S. Yang, J.A. Schwalbe, A.C. Nielander, J.M. McEnaney, K. Enemark-Rasmussen, J.G. Baker, A.R. Singh, B.A. Rohr, M.J. Statt, S.J. Blair, S. Mezzavilla, J. Kibsgaard, P.C.K. Vesborg, M. Cargnello, S.F. Bent, T.F. Jaramillo, I.E.L. Stephens, J.K. Nørskov, I. Chorkendorff, A rigorous electrochemical ammonia synthesis protocol with quantitative isotope measurements, NatureNature 570 (2019) 504–508, https://doi.org/10.1038/s41586-019-1260-x.
[26] S.M.M. Hizam, A.M. Al-Dhahebi, M.S. Mohamed Saheed, Recent advances in graphene-based nanocomposites for ammonia detection, Polymers. (Basel) 14 (2022) 5125, https://doi.org/10.3390/polym14235125.
[27] X. Cai, H. Iriawan, F. Yang, L. Luo, S. Shen, Y. Shao-Horn, J. Zhang, Interaction of ammonia with nafion and electrolyte in electrocatalytic nitrogen reduction study, J. Phys. Chem. Lett. 12 (2021) 6861–6866, https://doi.org/10.1021/acs.jpclett.1c01714.
[28] P. Arora, Z. (John) Zhang, Battery Separators, Chem. Rev. 104 (2004) 4419–4462, https://doi.org/10.1021/cr020738u.
[29] W. Xiao, Q. Yang, S. Zhu, Comparing ion transport in ionic liquids and polymerized ionic liquids, Sci. Rep. 10 (2020) 7825, https://doi.org/10.1038/s41598-020-64689-8.
[30] P.M. Jalbert, B. Commarieu, J.C. Daigle, J.P. Claverie, K. Zaghib, A 3D network based on poly(ε-caprolactone) macromonomers as polymer electrolyte for solid state lithium metal batteries, J. Electrochem. Soc. 167 (2020) 080527, https://doi.org/10.1149/1945-7111/ab8de0.
[31] C. Zhou, S. Bag, B. Lv, V. Thangadurai, Understanding the role of solvents on the morphological structure and li-ion conductivity of poly(vinylidene fluoride)-based polymer electrolytes, J. Electrochem. Soc. 167 (2020) 070552, https://doi.org/10.1149/1945-7111/ab7c3a.
[32] B. Izelaar, D. Ripepi, S. Asperti, A.I. Dugulan, R.W.A. Hendrikx, A.J. Böttger, F. M. Mulder, R. Kortlever, Revisiting the electrochemical nitrogen reduction on molybdenum and iron carbides: promising catalysts or false positives? ACS. Catal. 13 (2023) 1649–1661, https://doi.org/10.1021/acscatal.2c04491.
[33] J. Nørskov, J. Chen, R. Miranda, T. Fitzsimmons, R. Stack, Sustainable ammonia synthesis – exploring the scientific challenges associated with discovering alternative, sustainable processes for ammonia production, 2016. 10.2172/1283146.
[34] E. Murphy, Y. Liu, I. Matanovic, M. Rüscher, Y. Huang, A. Ly, S. Guo, W. Zang, X. Yan, A. Martini, J. Timoshenko, B.R. Cuenya, I.V. Zenyuk, X. Pan, E.D. Spoerke, P. Atanassov, Elucidating electrochemical nitrate and nitrite reduction over atomically-dispersed transition metal sites, Nat. Commun. 14 (2023) 4554, https://doi.org/10.1038/s41467-023-40174-4.
[35] D. Liu, L. Qiao, Y. Chen, P. Zhou, J. Feng, C.C. Leong, K.W. Ng, S. Peng, S. Wang, W.F. Ip, H. Pan, Electrocatalytic reduction of nitrate to ammonia on low-cost manganese-incorporated Co3O4 nanotubes, Appl. Catal. B 324 (2023) 122293, https://doi.org/10.1016/j.apcatb.2022.122293.
[36] M. Wang, S. Liu, H. Ji, T. Yang, T. Qian, C. Yan, Salting-out effect promoting highly efficient ambient ammonia synthesis, Nat. Commun. 12 (2021) 3198, https://doi.org/10.1038/s41467-021-23360-0.
[37] G. Zhou, T. Li, R. Huang, P. Wang, B. Hu, H. Li, L. Liu, Y. Sun, Recharged Catalyst with Memristive Nitrogen Reduction Activity through Learning Networks of Spiking Neurons, J. Am. Chem. Soc. 143 (2021) 5378–5385, https://doi.org/10.1021/jacs.0c12458.
[38] Y. Liu, X. Zhang, Z. Chen, X. Zhang, P. Tsiakaras, P.K. Shen, Electrocatalytic reduction of nitrogen on FeAg/Si for ammonia synthesis: a simple strategy for continuous regulation of faradaic efficiency by controlling H+ ions transfer rate, Appl. Catal. B 283 (2021) 119606, https://doi.org/10.1016/j.apcatb.2020.119606.
[39] L.M. Wilder, K. Wyatt, C.A. Skangos, W.E. Klein, M.R. Parimuha, J.L. Katsirubas, J. L. Young, E.M. Miller, Membranes matter: preventing ammonia crossover during electrochemical ammonia synthesis, ACS. Appl. Energy Mater. 7 (2024) 536–545, https://doi.org/10.1021/acsaem.3c02461.
[40] W. Bi, E. Gyenge, D.P. Wilkinson, Crossover, volatilization, and adsorption of ammonium ions in a proton-exchange membrane electrolyzer in relation to electrochemical ammonia production, Chem. Eng. J. 478 (2023) 147359, https://doi.org/10.1016/j.cej.2023.147359.
[41] F. Hanifpour, A. Sveinbjörnsson, C.P. Canales, E. Skúlason, H.D. Flosadóttir, Preparation of nafion membranes for reproducible ammonia quantification in nitrogen reduction reaction experiments, Angew. Chem. 132 (2020) 23138–23142, https://doi.org/10.1002/ange.202007998.
[42] M. Leonardi, G. Tranchida, R. Corso, R.G. Milazzo, S.A. Lombardo, S.M.S. Privitera, Role of the Membrane Transport Mechanism in Electrochemical Nitrogen Reduction Experiments, Membranes. (Basel) 12 (2022) 969, https://doi.org/10.3390/membranes12100969.
[43] J.J. Giner-Sanz, G. Leverick, V. Pérez-Herranz, Y. Shao-Horn, Optimization of the salicylate method for ammonia quantification from nitrogen electroreduction, J. Electroanal. Chemistry 896 (2021) 115250, https://doi.org/10.1016/J.JELECHEM.2021.115250.
[44] L. Zhang, X. Ji, X. Ren, Y. Ma, X. Shi, Z. Tian, A.M. Asiri, L. Chen, B. Tang, X. Sun, Electrochemical ammonia synthesis via nitrogen reduction reaction on a MoS 2 catalyst: theoretical and experimental studies, Adv. Mater. 30 (2018) 1800191, https://doi.org/10.1002/adma.201800191.
[45] J. Ingle, U.D. Patel, Electrochemical reduction of nitrate in the presence of silver-coated polyvinyl alcohol beads as a spatially suspended catalyst, J. Water. Process. Eng. 49 (2022) 103082, https://doi.org/10.1016/j.jwpe.2022.103082.
[46] M.A.A. Izquierdo-Gil, V.M.M. Barragán, J.P.G.P.G. Villaluenga, M.P.P. Godino, Water uptake and salt transport through Nafion cation-exchange membranes with different thicknesses, Chem. Eng. Sci. 72 (2012) 1–9, https://doi.org/10.1016/j.ces.2011.12.040.
[47] M. Schalenbach, L. Keller, B. Janotta, A. Bauer, H. Tempel, H. Kungl, M. Bonnet, R. A. Eichel, The Effect of Ion Exchange Poisoning on the Ion Transport and Conduction in Polymer Electrolyte Membranes (PEMs) for Water Electrolysis, J. Electrochem. Soc. 169 (2022) 094510, https://doi.org/10.1149/1945-7111/ac9087.
[48] A. Paspureddi, Z. Zhang, V. Ganesan, M.M. Sharma, L.E. Katz, Mechanism of monovalent and divalent ion mobility in Nafion membrane: an atomistic simulation study, J. Chem. Phys. 158 (2023), https://doi.org/10.1063/5.0145205.
[49] M.J. Kelly, G. Fafilek, J.O. Besenhard, H. Kronberger, G.E. Nauer, Contaminant absorption and conductivity in polymer electrolyte membranes, J. Power. Sources. 145 (2005) 249–252, https://doi.org/10.1016/j.jpowsour.2005.01.064.
[50] D. Johnson, A. Djire, Effect of pH on the Electrochemical Behavior and Nitrogen Reduction Reaction Activity of Ti 2 N Nitride MXene, Adv. Mater. Interfaces. 10 (2023), https://doi.org/10.1002/admi.202202147.
[51] X. Zhao, G. Hu, G. Chen, H. Zhang, S. Zhang, H. Wang, Comprehensive Understanding of the Thriving Ambient Electrochemical Nitrogen Reduction Reaction, Adv. Mater. 33 (2021), https://doi.org/10.1002/adma.202007650.
[52] T.F. Beltrame, F.M. Zoppas, J.Z. Ferreira, F.A. Marchesini, A.M. Bernardes, Nitrate reduction by electrochemical processes using copper electrode: evaluating operational parameters aiming low nitrite formation, Water Sci. Technol. 84 (2021) 200–215, https://doi.org/10.2166/wst.2021.215.
[53] N.C. Kani, A. Prajapati, B.A. Collins, J.D. Goodpaster, M.R. Singh, Competing Effects of pH, Cation Identity, H 2 O Saturation, and N 2 Concentration on the Activity and Selectivity of Electrochemical Reduction of N 2 to NH 3 on Electrodeposited Cu at Ambient Conditions, ACS. Catal. 10 (2020) 14592–14603, https://doi.org/10.1021/acscatal.0c04864.
[54] J. Peng, M. Tian, N.M. Cantillo, T. Zawodzinski, The ion and water transport properties of K+ and Na+ form perfluorosulfonic acid polymer, Electrochim. Acta 282 (2018) 544–554, https://doi.org/10.1016/j.electacta.2018.06.035.
[55] S. Cukierman, Et tu, Grotthuss! and other unfinished stories, Biochim. Biophys. Acta (BBA) Bioenergetics 1757 (2006) 876–885, https://doi.org/10.1016/j.bbabio.2005.12.001.
[56] T. Okada, N. Arimura, H. Satou, M. Yuasa, T. Kikuchi, Membrane transport characteristics of binary cation systems with Li+ and alkali metal cations in perfluorosulfonated ionomer, Electrochim. Acta 50 (2005) 3569–3575, https://doi.org/10.1016/j.electacta.2005.01.002.
[57] M. Saito, N. Arimura, K. Hayamizu, T. Okada, Mechanisms of ion and water transport in perfluorosulfonated ionomer membranes for fuel cells, J. Phys. Chem. B 108 (2004) 16064–16070, https://doi.org/10.1021/jp0482565.
[58] N.P. Berezina, N.A. Kononenko, O.A. Dyomina, N.P. Gnusin, Characterization of ion-exchange membrane materials: properties *vs* structure, Adv. Colloid. Interface Sci. 139 (2008) 3–28, https://doi.org/10.1016/J.CIS.2008.01.002.

[59] N.P. Gnusin, N.P. Berezina, N.A. Kononenko, O.A. Dyomina, Transport structural parameters to characterize ion exchange membranes, J. Memb. Sci. 243 (2004) 301–310, https://doi.org/10.1016/J.MEMSCI.2004.06.033.
[60] I.A. Stenina, P. Sistat, A.I. Rebrov, G. Pourcelly, A.B. Yaroslavtsev, Ion mobility in Nafion-117 membranes, Desalination. 170 (2004) 49–57, https://doi.org/10.1016/J.DESAL.2004.02.092.
[61] Y. Sone, P. Ekdunge, D. Simonsson, Proton Conductivity of Nafion 117 as Measured by a Four-Electrode AC Impedance Method, J. Electrochem. Soc. 143 (1996) 1254–1259, https://doi.org/10.1149/1.1836625/XML.
[62] A.V. Anantaraman, C.L. Gardner, Studies on ion-exchange membranes. Part 1. Effect of humidity on the conductivity of Nafion®, J. Electroanal. Chem. 414 (1996) 115–120, https://doi.org/10.1016/0022-0728(96)04690-6.
[63] L. Liu, W. Chen, Y. Li, An overview of the proton conductivity of Nafion membranes through a statistical analysis, J. Memb. Sci. 504 (2016) 1–9, https://doi.org/10.1016/J.MEMSCI.2015.12.065.